

Rheometers

Powder Rheology in Powder Bed-based Additive Manufacturing

Author

Philipp Beutler, Thermo Fisher Scientific,
Karlsruhe, Germany

Keywords

HAAKE MARS rheometer,
powder flow, additive manufacturing,
metal powders

Introduction

Additive manufacturing (AM) is a rapidly expanding field and has seen extensive interest from multiple industries. By adopting AM technologies, manufacturers can benefit from economically more attractive small batches of customized parts or direct production of 3D CAD models. Besides this, the layer-by-layer built-up of parts is less wasteful compared to traditional subtractive methods of production and for example in the case of metal powders, a recyclability of 95-98 % of the unused powder can be estimated.¹

Powder bed fusion (PBF) is a popular AM technique. This process involves sequentially spreading thin layers of powder over a build plate. Subsequently, a heat source is applied to selectively melt or sinter specific areas of the powder bed. To produce a homogeneous layer of powder, a good flowability is crucial. On the one hand, poor flowability can lead to discontinuities within the final product. On the other hand, the porosity of the spread layer is affected, which results in reduced mechanical strength and quality.²

Currently, the determination of *Hall* as well as *Carney* flowrate are popular methods to access flowability of AM powders. Here the time required for a certain amount of powder to flow through a calibrated orifice is measured. Despite being cheap and easy to work with, such funnel-based methods are highly operator dependent. Additionally, aeration of the powder can drastically affect the flowability through the orifice. Therefore, such techniques are best suited for simple comparative testing.³

As modern rheometers can be used to investigate the flowability of various samples, this application note intends to showcase the applicability of powder rheological techniques to access the flowability of various metal powders commonly used in PBF. Finally, the obtained results are compared with common determination methods of powder flowability by means of *Hall* and *Carney* flow.

Materials and methods

For this study, the flow behaviors of a titanium powder (Ti64), copper alloy powder (GRCop-42), and an aluminum alloy powder (AlSi10Mg), as well as two stainless steel powder batches (316L-A and recycled 316L-B) were investigated. Table 1 shows the key parameters D10, D50 and D90 of the particle size distribution as well as respective bulk density of each sample type. D10, D50 and D90 indicate the diameter at which 10 %, 50 % and 90 % of the particles are smaller.

Sample	D10 in μm	D50 in μm	D90 in μm	Bulk density in g/ml
Ti64	25.1	40	56.2	2.6
GRCop-42	17.0	27.2	40.2	4.2
AlSi10Mg	38.3	48.8	62.6	1.4
316L-A / 316L-B	18.8	28.8	40.9	4.2

Table 1. Particle size distribution and respective bulk densities of powder samples.

Particle sizes and bulk densities were determined following ISO 13322-2 and DIN EN ISO 3923-1, respectively.

To characterize the powder flowability of the powders, a Thermo Scientific™ HAAKE™ MARS™ iQ Rheometer equipped with the powder rheology measuring geometry was used. Figure 1 shows the setup used.

The powder flowability was characterized by a powder flow test, in which the resistance of the powder against the helical moving path of a vane rotor was recorded. This path is defined by a helix angle α as well as the tip speed v_{tip} of the vane rotor. Both parameters are controlled by the rheometer in form of an axial movement of the measuring head as well as the rotational speed of the vane rotor. This principle is illustrated in Figure 2.

This helical path in combination with the twisted shape of the rotor (blades) enables two different movement patterns. The first is a clockwise rotating downward movement, which is a typical sample conditioning step. This movement pattern removes stress and trapped air and results in a homogeneous, low stress packing state of the powder. The second is an anticlockwise rotating downward movement which causes high stress on and compression of the sample, and is therefore a typical test mode.

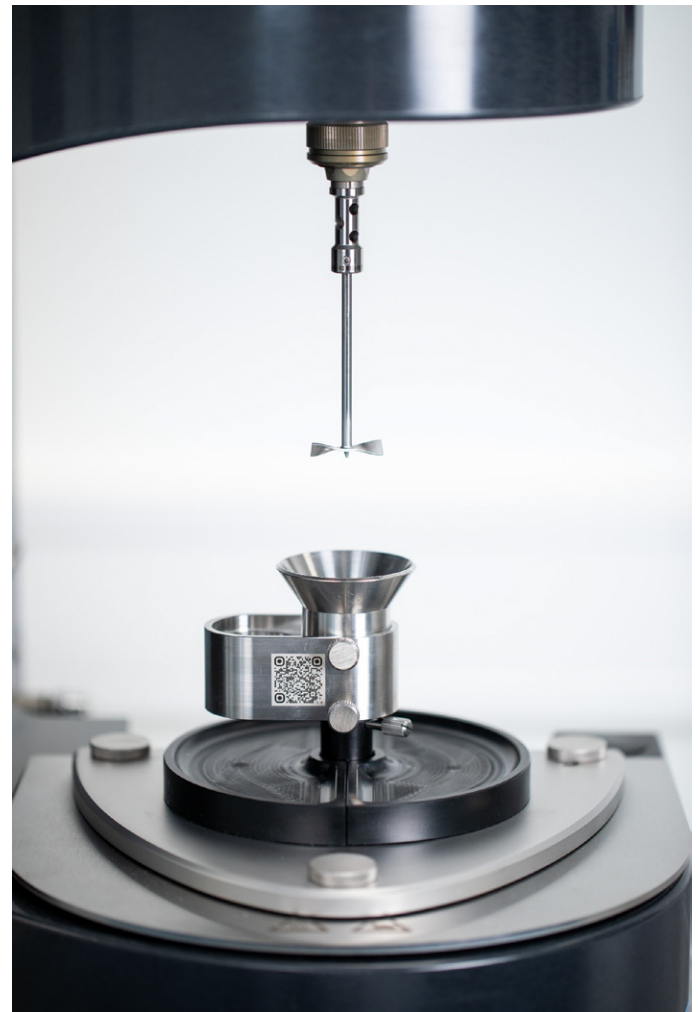


Figure 1. HAAKE MARS iQ Rheometer series with powder rheology accessory for powder flow measurements.

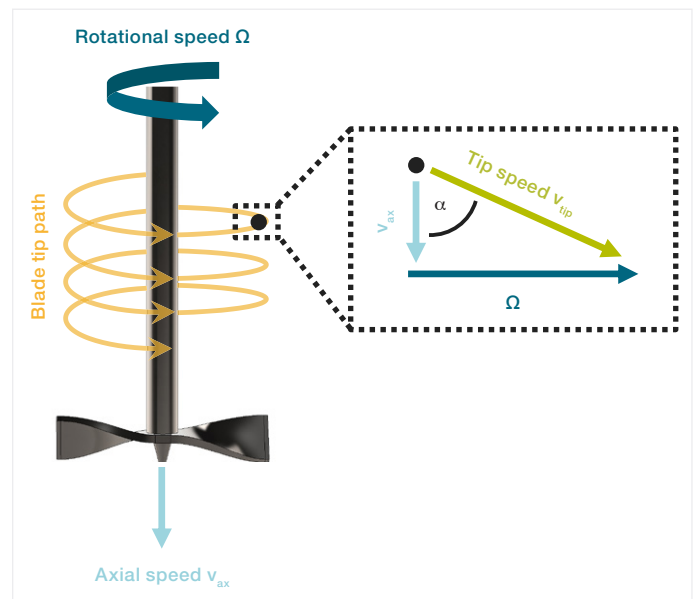


Figure 2. Movement principal a powder flow test.

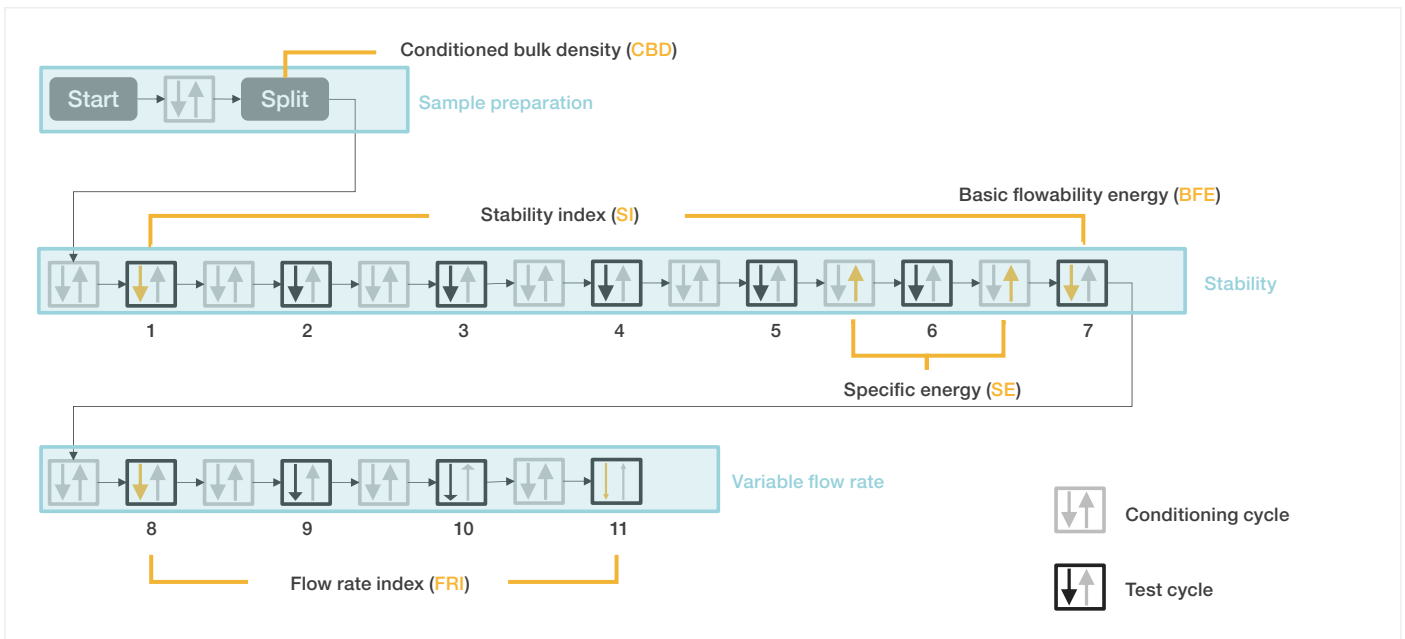


Figure 3. Schematic of complete powder flow measurement procedure.

The complete powder flow measurement procedure consists of several helical downward and upward movements of the rotor with several conditioning and test cycles. The entire test protocol is shown schematically in Figure 3 and can be divided into three parts.

In practice the sample is first loaded into the geometry up to the funnel (Figure 4 A) and an initial conditioning cycle with a tip speed of 40 mm/s is performed to remove all loading related stresses (Figure 4 B). This ensures that the test is operator-independent and that entrapped air is removed, avoiding possible aeration of the sample. After that, the sample split is performed by sliding the funnel sideways onto the reservoir to remove excess and to obtain a defined sample volume of 21.3 ml in the powder flow cup (Figure 4 C). By removing the cup from the triangular adapter plate and placing it on a scale (Figure 4 D), the powder mass can be obtained and entered in the Thermo Scientific™ HAAKE™ RheoWin™ Software to calculate the conditioned bulk density (CBD).

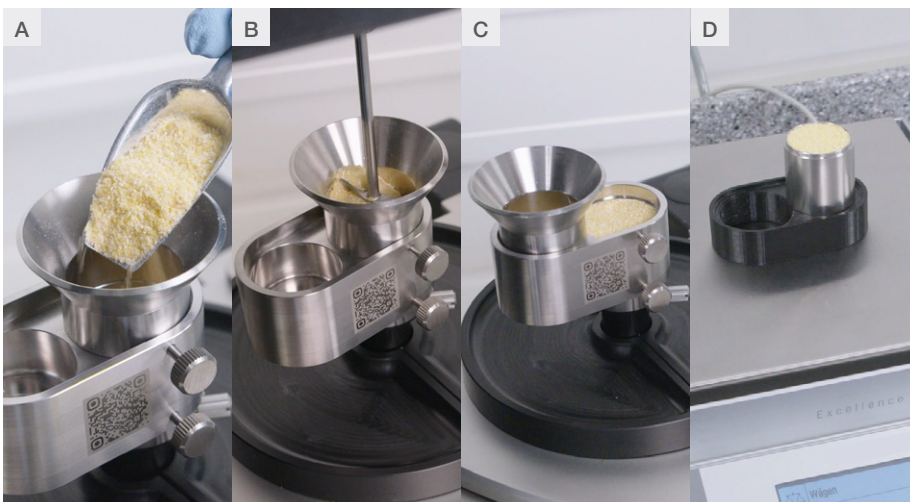


Figure 4. Images at various stages from the sample loading and conditioning procedure for powder flow tests.

Once the powder rheology geometry with the conditioned and weighed powder is installed again, the second part of the test, the stability measurement, is initiated. During this part a series of seven conditioning and test cycles is carried out. All conditioning cycles are performed with a tip speed of 40 mm/s to remove the stresses induced by previous cycles and all test cycles are conducted with 100 mm/s.

For evaluation, the HAAKE RheoWin software calculates the flow energy E_{flow} for the downward movement, based on the helix angle α used during the movement as well as the resistance of the powder against excitation in form of recorded normal force F_N and torque M according to equation (1). To account for the measuring geometry and the distance traveled during the test, the radius r as well as the start and end position h_{start} and h_{end} of for the path of the rotor are also incorporated in the calculation of the flow energy.

$$\text{Flow Energy} = \int_{h_{\text{start}}}^{h_{\text{end}}} \frac{M}{r \cdot \tan \alpha} + F_N dh$$

Equation 1.

During the second part of the powder flow measurement procedure, the stability of the powder during repeated testing is assessed by means of the stability index (SI) following equation (2).

$$\text{Stability Index (SI)} = \frac{\text{Flow energy test 7}}{\text{Flow energy test 1}}$$

Equation 2.

If a sample's SI value is around 1, a sample can be considered stable, and the flow energy of flow cycle 7 can be evaluated as basic flowability energy (BFE). Besides this, the specific energy (SE) can be derived from the 6th and 7th conditioning step of the stability test including the sample split mass with equation (3).

$$\text{Specific energy (SE)} = \frac{1}{2} \frac{\text{Upward conditioning energy test 6 + 7}}{\text{Sample split mass}}$$

Equation 3.

In contrast to the parameters mentioned before, the SE is a measure of energy needed to gently shear and lift conditioned powder during the upward movement of the rotor in the powder sample. This can be used to investigate the powder flow behavior in a low stress state regarding interlocking of particles due to different particle shapes of textures and cohesion.

The third and last part of the powder flow measurement consists of four alternating conditioning and test cycles in which the conditioning tip speed was set to 40 mm/s, whereas the tip speed of each test was decreased with each cycle starting from 100 mm/s and sequentially dropping to 70 mm/s, 50 mm/s and 25 mm/s. During this part of the procedure, the sensitivity of a powder to changes in flow rate can be described using the flow rate index (FRI) according to equation (4).

$$\text{Flow rate index (FRI)} = \frac{\text{Flow energy test 11}}{\text{Flow energy test 8}}$$

Equation 4.

The helix angle for all cycles was set to 5°. The respective HAAKE RheoWin measurement procedure is shown in Figure 5.

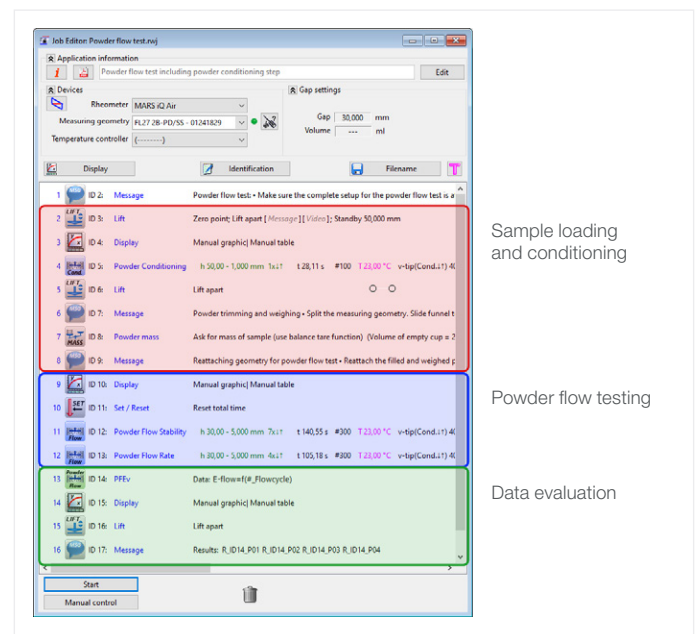


Figure 5. Powder flow measurement procedure in HAAKE RheoWin Software.

In addition to the tests described above, flowability data was also obtained by means of a Hall flow as well as Carney flow to benchmark the results from the powder flow measuring procedure with industry standards.

Results and discussion

Bulk Density

Bulk density (BD) is defined as ratio of the weight of the powder to its occupying volume including interparticle voids and is an important metric for accessing the properties of the final part. For example, when using powders with low bulk densities for PBF, final parts can have an increased surface roughness.²

An advantage of the powder flow measuring procedure is that one not only obtains certain parameters to evaluate powder flow but also gets information about CBD. Since the procedure involves conditioning steps and the powder flow cup has a defined volume, operator dependencies during sample filling or reading a value for the volume from a scale of a beaker can be eliminated. Figure 6 shows the comparison between BD from Table 1 and CBD.

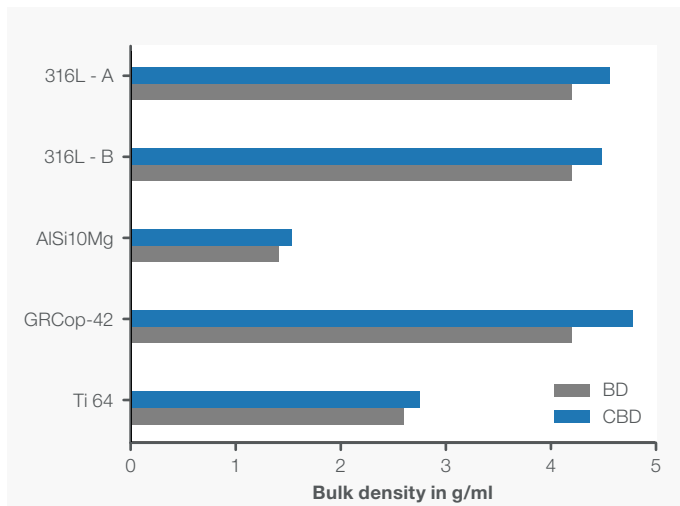


Figure 6. Comparison between bulk density (BD) and conditioned bulk density (CBD).

According to ISO 3923:1, BD is determined by the mass of powder flowing through a funnel into a cup of known volume. In contrast to this, CBD is determined from a conditioned state, in which the powder is gently loosened by the powder vane rotor to reach a homogeneously packed state with closer packed particles. Therefore, CBD is always higher compared to BD, ranging from a deviation of 5 % in the case of Ti64 up to 12 % for GRCop-42. However, both materials follow the same trend, leading to the conclusion that CBD is suitable for a comparative bulk density measurement for the powders in the scope of this study. A significant advantage of the determination of bulk density after conditioning over the funnel method is the operator independent way of conducting the test. Moreover, air entrapped during the flow of powder from the funnel into the cup can lead to an apparent increase in observed bulk density.

Powder flowability

For most powder flow-related evaluation parameters, only the downward movement of the vane rotor during the test cycle is of interest. Figure 7 shows the flow energies calculated from the torque as well as the normal force recorded during the helical movement.

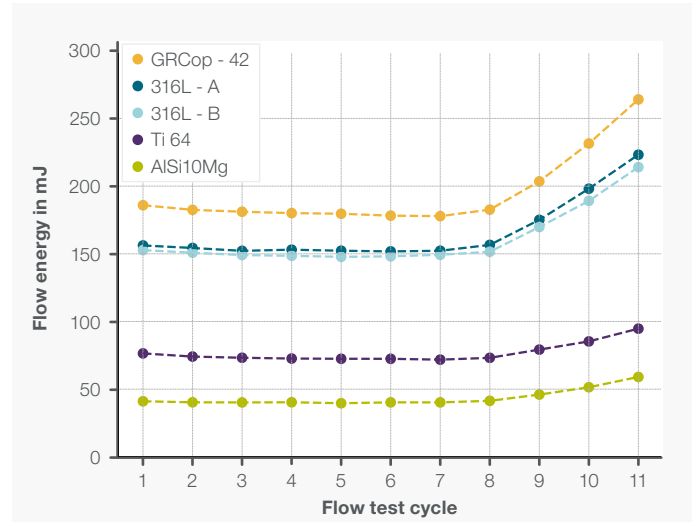


Figure 7. Calculated flow energies as a function of flow test cycle for each powder sample.

AlSi10Mg shows the overall lowest flow energy and can therefore be expected to be very flowable. This is unusual, as aluminum powders in general tend to agglomerate, resulting in poor flowability. To improve the flowability, the powder subject to this study was optimized by the manufacturer for additive manufacturing application. In contrast to this, GRCop - 42 can be characterized by the highest flow energies of all samples in this study and most likely as the least flowable.

All parameters derived from the powder flow measurements are displayed in Table 2.

Sample	BFE in mJ	SI	SE in mJ/g	FRI	Hall flowability in s/50 g	Carney flowability in s/50 g
Ti64	71.8	0.94	0.9	1.29	45.4	-
GRCop - 42	178	0.96	1.26	1.45	19	4
AlSi10Mg	40.2	0.98	0.98	1.43	44	10
316L-A	152	0.97	1.25	1.43	-	-
316L-B	149	0.98	1.22	1.41	-	-

Table 2. Evaluation parameters derived from the powder flow measurement as well as Hall and Carney flow.

All powder samples discussed in this study behave stably throughout the stability test. Hence, the SI for all powders is close to 1, indicating no electrostatic charging as well as no detectable powder friability.

Interestingly, the BFE seems to correspond well to the flowability obtained by both *Hall* and *Carney* flow, indicating that a high BFE translates to low *Hall* and *Carney* flowabilities. However, the Ti64 sample was not measured with the *Carney* funnel. Besides this, both 316L batches could also not be characterized with any funnel method as the powder did not flow through the orifice. Therefore, the powder flow measurement procedure was able to provide meaningful results for powders that were not entirely free-flowing.

In this study, most powders show an FRI in the range of 1.4. Only Ti64 appears to have a lower dependency of the flow on changes in tip speed. This could be related to less particle interlocking and hence less resistance against flow at different rates. Therefore, the flow behavior of Ti64 will not change as much when handled with different flow rates compared to other samples.

All powder flow related parameters discussed so far were obtained from confined flow conditions. This means that the powder has only limited space inside the powder flow cup to evade the compressing flow pattern of the vane rotor. Consequently, the sample is pushed downwards in front of the blade resulting in a relatively high stress state.

In contrast to this, the specific energy (SE) is determined from the upward movement of the vane rotor gently lifting powder particles and resulting in a low stress, unconfined flow. Hence, the main factor affecting the SE is the interlocking of particles in low stress flow. Like in the case of FRI, Ti64 also has the lowest SE, confirming that this powder shows less particle interlocking—possibly related to smoother particle shapes. Interestingly, AlSi10Mg also shows a significantly lower SE compared to 316L or GRCo-42; it is comparable to Ti64 which correlates with the BFE, where both samples have the lowest flow energy and *Hall* flowability. This is in accordance with literature, where BFE and SE were correlated with the irregular shape and particle interlocking of Ti64 powders.⁴

Together with other powder related parameters like particle shape and size distribution of particle surface properties, powder flow properties can be attributed to layer porosity, layer surface or layer packing density for parts manufactured by means of AM.²

Conclusion

In this application note, various types of metal powders were evaluated in terms of their flow behavior. The results of powder flow measurements were compared to bulk density as well as *Hall* and *Carney* flow measurements, and showed good agreement. Powder flow testing also allowed for testing samples that could not be analyzed by means of *Hall* or *Carney* flow.

Apart from being able to assess powder flowability in a way comparable to commonly used testing methods, the influence of particle interlocking due to particle shape and morphology on powder flowability can also be evaluated. Based on such findings, it is shown that by employing the proper rheometric instrumentation, powder performance for additive manufacturing processes can be evaluated, controlled and optimized.

Sources:

1. Ford, S. and Despeisse M. – Additive manufacturing and sustainability: an exploratory study of the advantages and challenges. *J. Clean. Prod.* (2016)
2. Talebi, F.A. et al. – Spreadability of powders for additive manufacturing: A critical review of metrics and characterization methods. *Particuology* (2024)
3. Schulze, D. – *Powder and Bulk Solids: Behavior, Characterization, Storage and Flow*, 1st Edition (2017)
4. Mehrabi M. et al. – An investigation of the effect of powder flowability on the powder spreading in additive manufacturing. *Powder Technology* (2023)

 Learn more at thermofisher.com/powder-rheology

thermoscientific